Journal of Hazardous Materials A116 (2004) 1–10

Journal of Hazardous Materials

www.elsevier.com/locate/jhazmat

Vented gaseous deflagrations: modelling of hinged inertial vent covers

V.V. Molkov*, A.V. Grigorash, R.M. Eber, D.V. Makarov

University of Ulster, FireSERT, Shore Road, Newtownabbey, Co. Antrim, Northern Ireland BT37 0QB, UK

Received 2 December 2003; received in revised form 3 August 2004; accepted 3 August 2004
Available online 19 October 2004

Abstract

The model of explosion pressure build up in enclosures with inertial vent covers and the CINDY code implementing the model are validated against experiments by Höchst and Leuckel (1998) in a 50 m^3 vessel with a pair of ceiling-mounted upwards-opening hinged doors in a 'butterfly' configuration with surface densities of 73 and 124 kg/m^2 under conditions of initially quiescent and turbulent mixtures. The model and the code are further validated against an experiment by Zalosh (1978) in a 33.5 m^3 room-like enclosure with a pair of wall-mounted rectangular doors, in a parallel configuration, each hinged at its bottom edge with a surface density of 23.1 kg/m^2 and initially quiescent mixture. A formula for the torque acting upon a rotating venting door is derived under conditions of vent cover jet formation. The vent cover jet effect decreases the torque three times compared to an elementary approach valid at the start of vent cover movement. It is demonstrated that, similar to translating vent covers, the vent cover jet effect is crucial for prediction of interdependent vent cover displacement in time and pressure transients.

Keywords: Explosion/deflagration; Inertial vent cover; Vent cover jet effect; Venting generated turbulence; Surface density/inertia

1. Introduction

The first theories of vented gaseous deflagration dynamics were developed by Yao [1] and Pasman et al. [2] in 1974 with the turbulence factor as a lumped parameter. A detailed theory of vented deflagration in spherical vessels was published by Bradley and Mitcheson [3] in 1978. In 1981, Molkov and Nekrasov [4] suggested a deflagration theory with two lumped parameters, i.e. the turbulence factor (χ) and generalized discharge coefficient (μ). This theory has been shown in the following years to predict the dynamics of gaseous deflagrations reasonably well for both closed and vented enclosures for a wide range of explosion conditions. The history of development of this model is outlined in Molkov [5]. Recently, Razus and Krause [6] published a comparative study of a number of lumped parameter models. They demonstrated that model compared favourably to its analogues in predicting explosion overpressures. In 2002, Hirano [7] presented the correlation for turbulence generated during vented deflagrations, published for the first time in [5]; in his invited paper, Williams [8] cited findings in scaling of explosions based on the model [9]. Russo and coworkers [10], in their study of pressure piling in connected vessels, demonstrated that only "the universal correlation by Molkov [11] for vent sizing at initially elevated pressures is quite able to reproduce almost all overpressures observed in the second vessel in 115 experiments". The accuracy of model predictions has been found to be significantly higher than predictions made using the approach offered in NFPA 68 [12] and [13].

Modifications to the model to account for translating inertial vent covers were presented recently in Molkov et al. [14]. Herein a derivation of the equations governing behaviour of hinged inertial covers will be presented. Discussion of the development of empirical coefficients supporting the hinged inertial vent model is also presented. Finally, the results of the model and the code validation against published experimental data are shown.

* Corresponding author. Tel.: +44 28 9036 8731; fax: +44 28 9036 8700.
E-mail address: V.Molkov@ulster.ac.uk (V.V. Molkov).

0304-3894/$ – see front matter © 2004 Elsevier B.V. All rights reserved.
doi:10.1016/j.jhazmat.2004.08.027

Nomenclature

a	radius of spherical vessel of equivalent volume (m)
A	fraction of cross-section area of vent occupied by burnt gas
A_{jet}	empirical coefficient
b	door length (m)
c_{ui}	speed of sound in gas (m/s)
C_{jet}	empirical coefficient
E_i	combustion products expansion coefficient at initial conditions
$f_{jet}(\varphi)$	transient factor
F	area (m^2)
g	acceleration gravity, 9.80665 m/s^2
H/D	ratio of height to diameter
$H \times W \times L$	height, width and length of enclosure
J_m	moment of inertia of the vent (kg m^2)
l	coordinate along door width, $0 \le l \le L$ (m)
L	door width (length of the pivoting side) (m)
M	molecular mass (kg/kmol)
m	mass (kg)
n	relative gas mass inside the vessel
p	pressure (Pa)
r_b	burnt gas equivalent sphere radius (m)
R	universal gas constant, 8314.4 J/K/kmol
R_Σ	outflow contribution
$R^\#$	outflow parameter
S_{ui}	mixture burning velocity at initial conditions (m/s)
t	time (s)
T	temperature (K)
T_{full}	full torque (N m)
$T_{gravity}$	torque exerted by the gas pressure on the hinged door (N m)
$T_{pressure}$	torque generated by the force of gravity (N m)
u_1	flow velocity through the vent cross-section (m/s)
u_L	flow velocity in the changing venting area (m/s)
V	enclosure volume (m^3)
w	inertia (surface density) (kg/m^2)
W_Σ	transient venting parameter
Z	auxiliary quantity

Greek

α	angular acceleration (radian/s^2)
ε	overall thermokinetic exponent
γ	ratio of specific heats
μ	generalized discharge coefficient
φ	angle of opening of a hinged door
χ	turbulence factor
π_0	pi number, 3.141593...
π	dimensionless pressure, p/p_i
ρ	density of gas (kg/m^3)
σ	dimensionless density, ρ/ρ_i
τ	dimensionless time, $=t\,S_{ui}/a$
ω	angular speed (radian/s)

Subscripts and superscripts

1	in the vent cross-section
a	at the atmospheric pressure level
b	burnt gases
closed	at closed door conditions
f	flame front
full	full torque
gravity	torque generated by the force of gravity
i	initial state
j	vent number, summation index
jet	pertaining to the jet effect
L	at changing venting area
new	new value at the end of the integration step
N	nominal, 100% open vent
pressure	gas pressure force
S	sphere
u	unburnt gases
v	venting, latching

2. Equations of vented deflagration dynamics for multiple vents

Derivation of the equations of vented gaseous deflagration dynamics for the case of a single non-inertial venting device was published in [4] and [5]. The derivation relied upon: conservation laws (mass, volume, energy), ideal gas state equation, and standard orifice equations for calculation of mass flow rate for subsonic and sonic regimes of outflow.

Ratio the real flame front area $F_f(t)$ at any moment t to the surface area $F_s(t)=4\pi_0 r_b^2$ of a sphere of radius r_b (where b, burnt gases; s, sphere and π_0, the number 'pi') to which burnt gas inside the enclosure could be gathered at the same moment. This ratio is called a turbulence factor $\chi(t)=F_f(t)/F_s(t)$. For the ideal case of laminar spherical flame propagation the turbulence factor is constant during the course of deflagration and equal $\chi = 1$. For real large-scale explosion problems values of χ two orders higher, i.e. up to 100, can be expected [15].

The simultaneous discharges from multiple vents add up, and that results in the following system of governing equations [16]:

$$\frac{d\pi}{d\tau} = 3\pi \frac{\chi(\tau)Z\pi^{\varepsilon+1/\gamma_u}(1-n_u\pi^{-1/\gamma_u})^{2/3} - \gamma_b W_\Sigma(\tau)R_\Sigma}{\pi^{1/\gamma_u} - (\gamma_u - \gamma_b/\gamma_u)n_u}, \quad (1)$$

$$R_\Sigma = R_u^\# \frac{\sum_j [1 - A_j(\tau)]\mu_j F_j(\tau)}{\sum_j \mu_j F_j(\tau)} + R_b^\# \left(\frac{\pi^{1/\gamma_u} - n_u}{n_b}\right) \frac{\sum_j A_j(\tau)\mu_j F_j(\tau)}{\sum_j \mu_j F_j(\tau)}, \quad (2)$$

$$\frac{dn_b}{d\tau} = 3\left[\chi(\tau)\pi^{\varepsilon+1/\gamma_u}(1 - n_u\pi^{-1/\gamma_u})^{2/3} - R_b^\# W_\Sigma(\tau)\frac{\sum_j A_j(\tau)\mu_j F_j(\tau)}{\sum_j \mu_j F_j(\tau)}\right], \quad (3)$$

$$\frac{dn_u}{d\tau} = -3\left[\chi(\tau)\pi^{\varepsilon+1/\gamma_u}(1 - n_u\pi^{-1/\gamma_u})^{2/3} + R_u^\# W_\Sigma(\tau)\frac{\sum_j [1 - A_j(\tau)]\mu_j F_j(\tau)}{\sum_j \mu_j F_j(\tau)}\right], \quad (4)$$

where π is the dimensionless pressure ($=p/p_i$, where i is the initial state, p is the pressure (Pa), p_i is the initial pressure in the vessel (Pa)), τ is the dimensionless time ($=t\,S_{ui}/a$, where S_{ui} laminar burning velocity at initial conditions (m/s) and a is the radius of spherical vessel of equivalent volume (m)), ε is the overall thermokinetic exponent, γ_u is the adiabatic exponent (ratio of specific heats) for unburnt mixture (where u is the unburnt gases), γ_b is the adiabatic exponent (ratio of specific heats) for burnt mixture (where b is the the burnt gases), n_u is the relative mass of unburnt mixture inside the vessel ($=m_u/m_i$, where m is the mass (kg)), n_b is the relative mass of burnt mixture inside the vessel ($=m_b/m_i$), A is the fraction of cross-section area of vent occupied by burnt gas (j is the vent number or summation index), μ_j is the generalized discharge coefficient for the jth vent, F is the vent area (m^2), R_Σ is the outflow contribution, where $R^\#$ is the outflow parameters (defined below), and Z is the auxiliary quantity:

$$Z = \gamma_b\left[E_i - \frac{\gamma_u}{\gamma_b}\frac{\gamma_b - 1}{\gamma_u - 1}\right]\pi^{1-\gamma_u/\gamma_u} + \frac{\gamma_b - \gamma_u}{\gamma_u - 1},$$

where E_i is the combustion products expansion coefficient at initial conditions. $W_\Sigma(\tau)$ is the transient venting parameter

$$W_\Sigma(\tau) = \frac{1}{\sqrt[3]{36\pi_0}\sqrt{\gamma_u}}\frac{c_{ui}}{S_{ui}}\frac{\sum_j \mu_j F_j(\tau)}{V^{2/3}},$$

where $c_{ui} = (\gamma_u R T_{ui}/M_{ui})^{1/2}$ is the speed of sound in unburnt gas (m/s) (where R = the universal gas constant (J/K/kmol), =8314.41; T_{ui} is the temperature of unburnt gas at initial conditions (K) and M_{ui} is the molecular mass of unburnt mixture at initial conditions (kg/kmol)), and V is the enclosure volume (m^3).

The outflow parameters $R_u^\#$ and $R_b^\#$ for unburned and burned mixture in Eqs. (1), (3) and (4) arise from the orifice equations and are calculated differently for subsonic and sonic flow conditions. For subsonic regime, the outflow parameter is equal to

$$R^\# = \left\{\frac{2\gamma}{\gamma - 1}\pi\sigma\left[\left(\frac{p_a}{p_i\pi}\right)^{2/\gamma} - \left(\frac{p_a}{p_i\pi}\right)^{(\gamma+1)/\gamma}\right]\right\}^{1/2} \quad (5)$$

and for sonic regime, it is equal to

$$R^\# = \left[\gamma\left(\frac{2}{\gamma + 1}\right)^{\gamma+1/\gamma-1}\pi\sigma\right]^{1/2}, \quad (6)$$

where σ is the relative density of gases (σ_u for unburnt gases, $=\rho_u/\rho_i = \pi_u^{1/\gamma}$; σ_b for burnt gases, $=\rho_b/\rho_i = \pi_b^{1/\gamma}$; ρ_u is the density of unburnt gases (kg/m^3); ρ_b is the density of burnt gases (kg/m^3); ρ_i is the initial density of unburnt gases (kg/m^3), $=m_i/V$) and p_a is the atmospheric pressure outside the vessel (Pa). The unburned and burned versions $R_u^\#$ and $R_b^\#$ of $R^\#$ are obtained from Eqs. (5) and (6) by substituting the unburnt and burnt versions of γ and σ in these formulae, respectively. The condition of transition from subsonic to sonic flow regime is

$$\pi \geq \frac{p_a}{p_i}\left(\frac{1 + \gamma}{2}\right)^{\gamma/\gamma-1} \quad (7)$$

Again, this is calculated separately for unburned and burned mixture, with γ_u and γ_b.

3. Modelling of hinged vent covers

Eqs. (1), (3) and (4) above depend on the current venting area that changes with time. The character of this change should be specified. This allows vent covers of any type to be ‘plugged in’ the calculations, as long as the value of the current venting area $F(t)$ can be calculated. For each vent cover, in conditions of pressure growing with time, at some moment t_{vj}, when the gas pressure is equal to the pre-set ‘latch release’ pressure p_{vj} (Pa), the release of vent cover ‘j’ occurs, and outflow of gases from the enclosure through the vent ‘j’ begins into the surrounding atmosphere. Depending on the vent cover type, the venting area either immediately becomes equal to the nominal vent area F_N (non-inertial vent covers, or rupture membranes) (where N is the nominal area) or increases gradually with time while vent cover moves away by the pressure force. The focus of this paper is on hinged covers. Translating covers are presented in our earlier paper [14].

A hinged ‘door’ or ‘cover’ is an inertial cover modelled as a solid rectangle able to swing about one of its edges, the hinge, fixed on the enclosure, e.g. as shown in Fig. 1.

3.1. Venting area

Denote b the length of the hinged side (m), i.e. the length of the door; L the length of the pivoting side (m), i.e. the width of the door. Then the nominal area of the vent opening and the area of the hinged door is $F_N = bL$. It is further assumed that the vent cover mass is distributed uniformly over the surface of the cover, with surface density or inertia w (kg/m^2). Let φ be the angle between the vent opening and the hinged door. It is assumed that the current venting area $F(\varphi)$ is the gap area between the edges of the cover and the vent opening. The gap, as shown in Fig. 1, is formed from one rectangular region, based on the door edge opposite to the hinge and two triangular regions, based on the pivoting edges of the door. The venting area is then:

$$F(\varphi) = \min\left\{F_{\mathrm{N}}, 2L\sin\left(\frac{\varphi}{2}\right)\left[b + L\cos\left(\frac{\varphi}{2}\right)\right]\right\} \quad (8)$$

This area is zero for a closed vent ($\varphi = 0$) and is allowed to increase until $\varphi = \varphi_{\mathrm{N}}$; it reaches the maximum value equal to the nominal vent area F_{N}. Also assume that for angles $\varphi > \varphi_{\mathrm{N}}$, the venting area stays equal to F_{N}. Furthermore, assume that the door is inelastically arrested at $\varphi = 90°$.

3.2. Pressure distribution for $F(\varphi) \leq F_N$

When the vent is closed, the gas pressure is uniform throughout the door surface, and is equal to $p(t)$, the pressure inside the enclosure (Pa). Furthermore, the gas mass discharge rate is zero. When the vent is open, the picture changes. First, the static pressure of the escaping gases on the door is smaller than the pressure at ‘stagnation’ conditions inside the enclosure. Second, the pressure is not uniform along the door surface any more.

The first issue is addressed by using the Bernoulli or mass conservation law for the gas flowing between the enclosure inside the vent cross-section and the current venting area. At the vent cross-section, let $p = p_1$, and $u = u_1$ (where u_1 is the flow velocity through the vent cross-section (m/s)), and flows are low enough to warrant the assumption of incompressibility. The Bernoulli’s equation for these two levels allows p_1 to be expressed as:

$$p_1 = p(t) - \frac{\rho\, u_1^2}{2}, \quad (9)$$

where ρ is the gas density constant (kg/m^3).

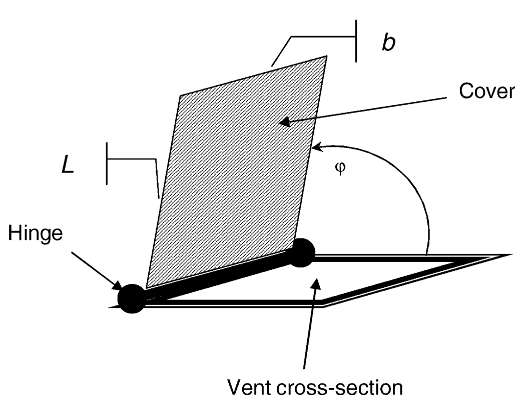

Fig. 1. Hinged door.

Outside the vessel the gas pressure is $p = p_{\mathrm{a}}$, and the average gas velocity in the changing venting area is $u = u_{\mathrm{L}}$. From the Bernoulli’s equation relating the inside and the outside of the vessel, u_{L} can be expressed as:

$$u_{\mathrm{L}} = \left\{\frac{2(p(t) - p_{\mathrm{a}})}{\rho}\right\}^{1/2} \quad (10)$$

The mass conservation law between the vent opening and the outside of the vessel gives an expression for u_1:

$$u_1 = \frac{u_{\mathrm{L}} F(\varphi)}{bL} \quad (11)$$

Substituting (10) in (11) and the results in (9) the pressure p_1 in the vent cross-section becomes

$$p_1 = p(t) - (p(t) - p_{\mathrm{a}})\frac{F^2(\varphi)}{(bL)^2} \quad (12)$$

This pressure depends on both the current explosion pressure and the current angle of the door opening.

The second issue is dealt with by assuming that the pressure along the door surface changes as a linear function of the position on the width of the door:

$$p(l, t) = p_1 - \frac{p_1 - p_{\mathrm{a}}}{L} l \quad (13)$$

Here $l \leq L$ is the current position, and p_1 is defined by (12). The assumption of a linear pressure distribution along the width of an inertial hinged vent cover is a simplification of a more complex three-dimensional distribution. A simple modelling including a portion of an enclosure, hinged vent cover, and a portion of the surrounding environment, was performed using Fluent$^{\mathrm{TM}}$. A constant internal pressure of 1.3 atm and external pressure of 1.0 atm were assumed. The problem was solved using a 2D approach, and the steady pressure distribution along the cover was determined for several cover opening angles. The results are shown in Fig. 2. Ultimately

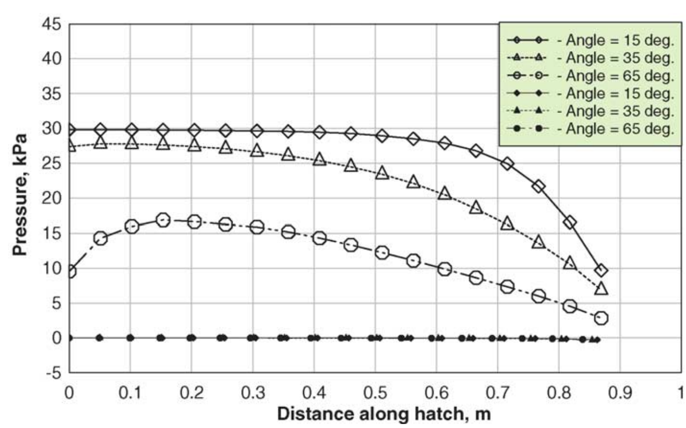

Fig. 2. Pressure distribution on inertial hinged vent cover as a function of cover opening angle for constant enclosure pressure. Steady-state problem, $p/p_0 = 1.3$, 2D segregated solver, k–ε turbulence model, ◊,△,◯—transients ‘below’ the cover, i.e. at cover surface hit by the escaping gases; ♦,▲,●—transients ‘above’ the cover.

a three-dimensional modelling, using CFD, will be necessary to accurately determine the pressure distribution on the hinged cover. As a first approximation, however, a linear distribution will force the model cover displacement to more closely match experimental experience than a model assuming the enclosure pressure everywhere on the cover.

3.3. Pressure force torque for $F(\varphi) \le F_N$

The torque exerted by the gas pressure on the door is (N m):

$$T_{\text{pressure}} = \int_0^L [p(l,t) - p_{\text{a}}]\, bl\, \mathrm{d}l \tag{14}$$

The pressure torque is always positive, since the gas flow momentum always works for opening the vent. Using formulae (12) and (13) by substitution in (14), the torque the gas applies to turn the door on its hinge can be written as:

$$T_{\text{pressure}} = \frac{bL^2}{6}[p(t) - p_{\text{a}}]\left(1 - \frac{F^2(\varphi)}{(bL)^2}\right) \tag{15}$$

Our assumption of linear change of pressure in (13) results in very easy derivations. However, the true pressure distribution is not linear, the whole vent cover-pushing phenomenon being three-dimensional, non-stationary and dependent on the geometry of the cover and vent opening. Therefore, we decided to settle on the linear distribution augmented by an empirical 'jet factor' C_{jet} as follows:

$$T_{\text{pressure}} = \frac{bL^2}{6C_{\text{jet}}}[p(t) - p_{\text{a}}]\left(1 - \frac{F^2(\varphi)}{(bL)^2}\right) \tag{16}$$

The C_{jet} will compensate for the true non-linear, non-stationary and geometry-dependent character of the hinged door movement.

Notice that when the door is closed, $\varphi = 0$, formula (15) gives three times smaller value than the correct torque for the closed door should be:

$$T_{\text{pressure,closed}} = \frac{bL^2}{2}[p(t) - p_{\text{a}}] \tag{17}$$

Therefore, we have to use different formulae for a closed or almost closed door and a sufficiently wide open door. When the door is shut or is opened within some small range of angles, we apply formula (17). Above a certain angle, when $F(\varphi)$ reaches a certain fraction A_{jet} of the full area bL, the velocity of gases escaping along the door surface becomes significant, and we have to apply formula (16). To ensure the continuity of transition from the 'pressure' regime of formula (17) to the 'jet' regime of formula (16), we assume this transition to be linear with respect to $F(\varphi)$ and controlled by the 'jet fraction' parameter A_{jet}. We also have to ensure that formula (16) never produces a value greater than formula (17) for the same pressure and cover dimensions. To that end, we restrict the values of the 'jet factor' by the condition $C_{\text{jet}} > 1/3$. With these considerations in mind, it is possible to replace (16) and (17) with a single formula

$$T_{\text{pressure}} = \frac{bL^2}{6 f_{\text{jet}}(\varphi)}[p(t) - p_{\text{a}}]\left(1 - \frac{F^2(\varphi)}{(bL)^2}\right), \tag{18}$$

where the transient factor $f_{\text{jet}}(\varphi)$ is

$$f_{\text{jet}}(\varphi) = \min\left\{\max\left(\frac{1}{3}, \frac{C_{\text{jet}} F(\varphi)}{bL A_{\text{jet}}}\right), C_{\text{jet}}\right\} \tag{19}$$

Indeed, when $\varphi = 0$, we have $F(\varphi) = 0$, the transient factor $f_{\text{jet}}(\varphi)$ equals 1/3, and formula (18) assumes the form of (17). At a certain angle φ, when $F(\varphi) = A_{\text{jet}} bL$, $f_{\text{jet}}(\varphi)$ becomes equal to C_{jet}, and stays at this value for any greater angle of opening. Respectively, formula (18) assumes the form of (16). For all the interim angles, formula (19) produces interim values of $f_{\text{jet}}(\varphi)$ between 1/3 and C_{jet}.

The values for the controlling parameters A_{jet} and C_{jet} have to be determined empirically. If comparison with an experiment shows that A_{jet} assumes relatively low values, say less than 10% of the nominal area, and C_{jet} turns out to be reasonable, say less than two, then formula (18) may be deemed a plausible approximation of the physical reality.

3.4. Balance of torques for $F(\varphi) \le F_N$

In rotational movement of our hinged door, the balance of torques (moments about the axis of rotation) can be expressed as follows:

$$T_{\text{full}} = T_{\text{pressure}} + T_{\text{gravity}} \tag{20}$$

where T_{full} is the full torque, T_{pressure} is the torque generated by the pressure of escaping gases, formula (18), and T_{gravity} is the torque generated by the force of Earth's gravity.

The full torque (N m) is $T_{\text{full}} = J_{\text{m}} \times \alpha$, where α is the angular acceleration of the vent (radian/s^2) and J_{m} is the moment of inertia of the vent (kg m^2). The general formula for J_{m} (kg m^2) is $J_{\text{m}} = \int_m l^2\, \mathrm{d}m$, where d$m$ is the elementary mass (kg) forming the body, and l is the distance of this elementary mass from the axis of rotation (hinge) (m). With the assumption of uniform mass distribution over the vent surface, the result is: $\mathrm{d}m = w\mathrm{d}F$, where w is the inertia of vent cover and dF is the area of a surface element. Then

$$J_{\text{m}} = w \int_{F_{\text{N}}} l^2 \mathrm{d}F$$

Since the vent is rectangular, this integral can be rewritten as

$$J_{\text{m}} = wb \int_0^L l^2 \mathrm{d}l = \frac{wbL^3}{3}$$

As the inertia w is expressed as $w = m/(bL)$ where m = mass (kg), the moment of inertia simplifies to

$$J_{\mathrm{m}} = \frac{mL^2}{3}$$

The full torque is therefore

$$T_{\mathrm{full}} = \frac{\alpha m L^2}{3}$$

The torque T_{gravity} of the gravity force depends on where the vent is mounted and what side of the vent is hinged. If the vent is mounted on a wall, and is hinged at its side edge, such that its swinging motion is in the horizontal plane, then $T_{\mathrm{gravity}} = 0$.

If the vent is mounted on a wall, and is hinged at its top edge, then

$$T_{\mathrm{gravity}} = -\frac{mgL\sin(\varphi)}{2},$$

where g is the acceleration gravity (m/s^2). T_{gravity} is negative because for a top-hinged wall-mounted vent the gravity works against the opening vent. If the vent is bottom-hinged to a wall, then the difference is only in the sign

$$T_{\mathrm{gravity}} = +\frac{mgL\sin(\varphi)}{2},$$

since gravity helps the vent to open in this case.

Analogously, if the vent is mounted on the ceiling and opens upwards, then

$$T_{\mathrm{gravity}} = -\frac{mgL\cos(\varphi)}{2},$$

and for vents mounted in the floor and opening downwards,

$$T_{\mathrm{gravity}} = +\frac{mgL\cos(\varphi)}{2}$$

For wall-mounted vents, gathering formula (18) and the above formulae for the torques in the Eq. (20) yields:

$$\frac{\alpha m L^2}{3} = \frac{bL^2(p(t) - p_{\mathrm{a}})}{6 f_{\mathrm{jet}}(\varphi)}\left(1 - \frac{F^2(\varphi)}{(bL)^2}\right) - \frac{mgL\sin(\varphi)}{2}, \qquad (21)$$

with a little change in notation for g. We assign the 'direction' for the gravitational force, such that $g > 0$ corresponds to the situation when the hinged edge is at the top; $g < 0$ when the hinged edge is at the bottom; and $g = 0$ when the hinged edge is at a side.

In a similar way, for ceiling/floor-mounted vents, $\sin\varphi$ in formula (21) should be changed to $\cos\varphi$, and it is assumed that $g > 0$ for ceiling-mounted vents that open upwards; $g < 0$ for floor-mounted vents that open downwards; and $g = 0$ for gravity compensated for by a spring or a balance.

A simple algebra in Eq. (21) yields the following formula for the angular acceleration of the vent. For a wall-mounted vent,

$$\alpha = \frac{3.0}{2.0}\left\{\frac{b\,(p(t) - p_{\mathrm{a}})}{m3 f_{\mathrm{jet}}(\varphi)}\left(1 - \frac{F^2(\varphi)}{(bL)^2}\right) - \frac{g}{L}\sin(\varphi)\right\},$$

and for a ceiling-mounted vent, $\sin(\varphi)$ should be changed to $\cos(\varphi)$.

The angular speed ω (radians/s) and the angle of opening φ (radians), are

$$\omega(t) = \int_0^t \alpha(\tau)\mathrm{d}\tau \quad \text{and} \quad \varphi(t) = \int_0^t \omega(\tau)\mathrm{d}\tau, \quad \text{respectively.}$$

Within each step of numerical integration of the governing equations, the angular acceleration is assumed constant. Therefore, uniformly accelerated motion formulae are used to obtain the new values ω_{new} and φ_{new} of the angular speed and the angle of opening at the end of the integration step from the values at the beginning of this step: $\omega_{\mathrm{new}} = \omega + \alpha\,\mathrm{d}t$ and $\varphi_{\mathrm{new}} = \varphi + \omega\,\mathrm{d}t + \alpha\,\mathrm{d}t^2/2.0$. At the end of each integration step the following assignments take place: $\omega = \omega_{\mathrm{new}}$; $\varphi = \varphi_{\mathrm{new}}$.

3.5. Torque when $F(\varphi) > F_N$

The applicability of formula (18) is limited in the angle φ of the door opening, in that the formula will work only under the assumption that the current venting area $F(\varphi)$ is less than the nominal area F_{N}.

At a certain angle φ_{N} such that $F(\varphi_{\mathrm{N}}) = F_{\mathrm{N}}$ the pressure at the vent cross-section is equal to the atmospheric pressure, and the gas flow through the vent is unrestricted, as though there had been no vent cover at all. The CINDY code assumes, when this point is reached, that the vent cover displacement continues; yet the energy imparted to the cover through momentum earlier in the deflagration is affecting cover motion. Since the primary interest in the current research was in the influence of vent cover inertia while the cover position and displacement could influence transient enclosure pressures, detailed analyses of cover displacement once the vent was found to be 100% opened have been neglected. Further modelling would be required to assure an accurate representation of cover behaviour.

4. Comparison with experiments

4.1. Values of the empirical coefficients

The empirical coefficients C_{jet} and A_{jet} in formula (19) were determined through matching of CINDY simulations of Höchst and Leuckel [17] experiments 3-B and 3-D ('experiment 3-B' or '3-B' denotes experimental results plotted in Fig. 3b of their paper; 'experiment 3-D' or '3-D' denotes experimental results plotted in Fig. 3d of their paper). A_{jet} for hinged covers represents a threshold below which jetting

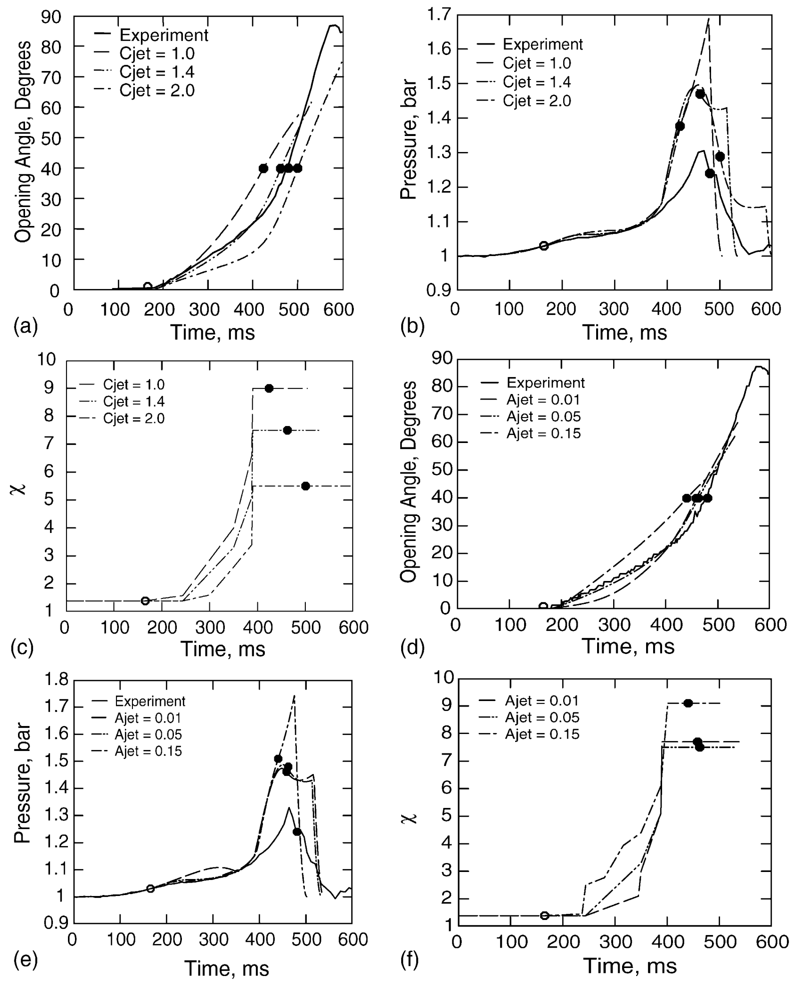

Fig. 3. (a) C_{jet}—Höchst and Leuckel, experiment 3-B: opening angle, $A_{jet} = 0.05$, $\mu = 1.2$ (○—vent starts to open, ●—vent 100% open). (b) C_{jet}—Höchst and Leuckel, experiment 3-B: pressure, $A_{jet} = 0.05$, $\mu = 1.2$ (○—vent starts to open, ●—vent 100% open). (c) C_{jet}—Höchst and Leuckel, experiment 3-B: χ, $A_{jet} = 0.05$, $\mu = 1.2$ (○—vent starts to open, ●—vent 100% open). (d) A_{jet}—Höchst and Leuckel, experiment 3-B: opening angle, $C_{jet} = 1.4$, $\mu = 1.2$ (○—vent starts to open, ●—vent 100% open). (e) A_{jet}—Höchst and Leuckel, experiment 3-B: pressure, $C_{jet} = 1.4$, $\mu = 1.2$ (○—vent starts to open, ●—vent 100% open). (f) A_{jet}—Höchst and Leuckel, experiment 3-B: χ, $C_{jet} = 1.4$, $\mu = 1.2$ (○—vent starts to open, ●—vent 100% open).

flows of gases escaping through the opening vent are assumed to not yet be established. The variation of the vent cover displacement and the enclosure pressure for varying C_{jet}, assuming constant values of A_{jet}, are shown in Fig. 3a and b for displacement and pressure, respectively (in these and following figures simulated curves are shown until the moment of full burnout of the mixture inside enclosure). Once the values for the coefficients were selected, the values of χ and μ to backfit the simulations to the experimental data were found. Fig. 3c shows the backfitted values of χ that were found (results were obtained with a constant discharge coefficient $\mu = 1.2$). As the figures show, increasing C_{jet} decreases the amount of force applied to the door—so the door takes longer to open. A slower opening door ‘generates’ less enclosure turbulence—thus the reductions in turbulence with increasing C_{jet}, as shown in Fig. 3c. The best fit seems to come with a value of C_{jet} of 1.4.

A similar process, holding C_{jet} constant, was used to explore the impact of varying A_{jet}. Fig. 3d and e compares computed and experimental displacements and pressures, respectively, for different values of A_{jet}, while Fig. 3f shows the resultant turbulence levels corresponding to the selected values of A_{jet}. For A_{jet} values at or below 0.01, the pressure is overestimated, yet the cover is not moving fast enough. Thus, values of A_{jet} at or below 0.01 should not be used. However, values of A_{jet} from 0.05 to 0.10 could be successfully used, although the turbulence rises as A_{jet} rises (Fig. 3f). As the figures show, increasing A_{jet} (in effect the amount of time the door is exposed to enclosure rather than door jetting conditions), ‘increases’ enclosure turbulence—the cover opens faster. The best fit seems to be achieved at an A_{jet} of 0.05.

Note that given the data shown in Fig. 3, an estimation of the sensitivity of the enclosure turbulence to the A_{jet} and C_{jet} may be estimated. An average shift in χ as A_{jet} or C_{jet} varies may be determined by observing the shift in χ in the backfitted curves, and comparing the shift that occurs for various values of the coefficients. As a result, it was calculated that

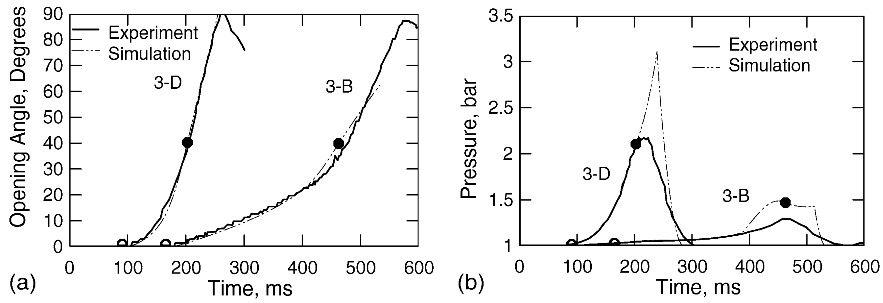

Fig. 4. (a). Höchst and Leuckel, experiments 3-B, 3-D: opening angle, $\mu = 1.2$ (◯–vent starts to open, ●–vent 100% open). (b). Höchst and Leuckel, experiments 3-B, 3-D: pressure, $\mu = 1.2$ (◯—vent starts to open, ●—vent 100% open).

when A_{jet} shifts ±10%, χ shifts ±1.5%. Similarly, when C_{jet} shifts ±10%, χ shifts in opposite direction ±6%. From this, it would seem that the enclosure turbulence is more sensitive to the amount of force applied to the vent cover than to the amount of time that force is applied.

The discrepancies between the experimental and simulation results in pressure dynamics, especially those in the peak areas, could be explained by heat losses to enclosure walls, which were not modelled in this study. From explosion safety engineering point of view it is acceptable as calculated pressure peaks are conservative relative to experimental data.

4.2. Validation 1: Höchst and Leuckel's experiments

The model has been validated against Höchst and Leuckel's experiments [17]. For translation panels, a detailed description of that validation was presented in [14]. Their apparatus consisted of a 50 m^3 silo of reinforced concrete with $H/D = 4$. The vent covers for these experiments were a pair of hinged vent covers arranged in a 'butterfly' configuration on the top surface of the silo. The edge of each cover most remote from the hinges was padded so that when the covers opened to 90°, the impact of the covers on each other was minimised. Experiment 3-B was a quiescent mixture of 10.7% methane–air, with a total venting area (for the two covers) $F = 1.91$ m^2, an inertia $w = 124$ kg/m^2, and torque of 532 N m. Experiment 3-D was a turbulent mixture (mixed by a fan within the enclosure for the purpose) of 10.6% methane–air, with a total venting area (for the two covers) $F = 1.91$ m^2, an inertia $w = 73$ kg/m^2, and torque of 314 N m. The mixtures were ignited by an electric match with energy of 75 J, located 3.5 m from the floor at the silo centre line. S_{ui} was 0.38 m/s; E_i was 7.4; γ_u was 1.39; γ_b was 1.25;c_{ui} was 353 m/s; F was 2.45 m^2; ε was 0.3; and the molecular mass (M) was 27.24 kg/kmol.

Fig. 4a compares the calculated opening angle transients with the experimental results, while Fig. 4b compares the calculated enclosure pressures with the experimental results. A good match of both displacement and pressure has been achieved, using the C_{jet} and A_{jet} coefficient values of 1.4 and 0.05, respectively. As expected, the pre-mixed enclosure gases in experiment 3-D results in faster opening of the cover, and higher and earlier pressures than those experienced by the quiescent mixture in experiment 3-B. These results are well matched by the CINDY computations. Fig. 5 shows how χ varied as the calculations progressed, and the best fit values of χ for experiments 3-B and 3-D. The enclosure gases were initially turbulent in experiment 3-D—thus the higher χ was needed to backfit the pressure and displacement are not surprising.

In the CINDY code, χ is implemented as piecewise-linear; over some ranges of backfitted values, many small increments in χ can be replaced by a few longer segments with little or no detrimental change to the backfit for either pressure or displacement. Data from future experiments will be required to further determine if a two- or three- step χ curve established by simple rules could predict deflagration dynamics.

4.3. Validation 2: Zalosh's experiment

The model has also been validated against an experiment of Zalosh [18]. His apparatus consisted of a rectangular concrete bunker with interior dimensions $H \times W \times L = 3.1$ m $\times$ 2.0 m $\times$ 5.4 m and a volume of 33.5 m^3. The only relief was a pair of wall-mounted blowoff panels, arranged vertically in parallel, hinged on the bottom edges, opening outwards and downwards, arrested by cables in the 90° opened position. Each door was sized to be 1.29 m^2, for a total venting area of 2.58 m^2. An initially quiescent near stoichiometric 10.0% mixture was ignited by a 12 J spark

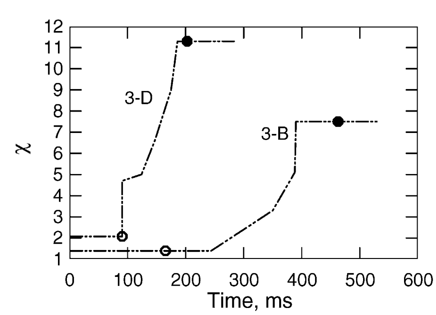

Fig. 5. Höchst and Leuckel, experiments 3-B, 3-D: χ, $\mu = 1.2$ (◯—vent starts to open, ●—vent 100% open).

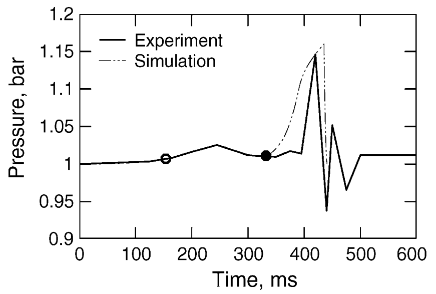

Fig. 6. Zalosh: pressure, $\mu = 1.2$ (○—vent starts to open, ●—vent 100% open).

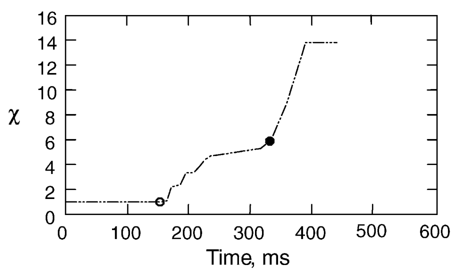

Fig. 7. Zalosh: χ, $\mu = 1.2$. (○—vent starts to open, ●—vent 100% open).

located in the centre of the bunker. In the calculations, the burning velocity, S_u, was 0.38 m/s; the combustion products expansion coefficient at initial conditions, E_i, was 7.4; the unburnt mixture adiabatic exponent, γ_u, was 1.39; the burnt gas adiabatic exponent, γ_b, was 1.25; the speed of sound, c_{ui}, was 353 m/s; the overall thermokinetic exponent, which gives the dependence of burning velocity on pressure at adiabatic compression conditions, ε, was 0.3; and the molecular mass, M, was 27.56 kg/kmol. Coefficient values of $C_{jet} = 1.4$ and $A_{jet} = 0.05$, determined by comparisons with experiments by Höchst and Leuckel [17], were used.

Fig. 6 compares the calculated pressure transients with the experimental results for hinged covers. No displacement data were published in Zalosh [18], so there is only a pressure comparison. The comparison to the experimentally observed pressure is reasonable. Fig. 7 shows how χ varied as the deflagration progressed, and the best fit values of χ for the experiment. The pressure rise at the end of the experiment seems to be due to turbulisation at the end of the process and a significant increase in χ is required to match the pressure.

5. Conclusions

- Modelling of vented deflagrations with inertial venting devices has been performed for the case of multiple hinged doors.
- The developed model and the CINDY code have been validated against large-scale experiments of Höchst and Leuckel [17] and Zalosh [18]. Good matches in both explosion overpressure transients and cover displacement transients have been achieved.
- The obtained empirical coefficients C_{jet} and A_{jet} assume plausible values of 1.4 and 0.05. Deviation of the empirical parameters C_{jet} and A_{jet} from values derived herein results in only small variances in the backfitted values of the turbulence factor χ.
- Observation of gradually changing turbulence factor χ over the processed experiments suggests that χ may be capable of being represented by a simple curve. The processing of additional experimental pressure and displacement test data would be useful to assess how predictable the gradual change of χ may be.

Acknowledgements

The authors wish to thank Dr. Siegfried Höchst for providing additional information about the structure of the vent panel arresting mechanisms used in the experiments he performed with Dr. Wolfgang Leuckel. Funding by the Engineering and Physical Sciences Research Council (EPSRC) through Grant #GR/R53333/01 is gratefully acknowledged.

References

[1] C. Yao, Explosion venting of low-strength equipment and structures, Loss Prev. 8 (1974) 1–9.
[2] H.L. Pasman, Th.M. Groothuizen, H. de Gooijer, Design of pressure relief vents, in: C.H. Buschman (Ed.), Loss Prevention and Safety Promotion in the Process Industries, New York, 1974, pp. 185–189.
[3] D. Bradley, A. Mitcheson, The venting of gaseous explosions in spherical vessels, Combust. Flame 32 (1978) 221–236, 237-255.
[4] V.V. Molkov, V.P. Nekrasov, Dynamics of gas combustion in a constant volume in the presence of exhaust, Combust. Explosion Shock Waves 17 (4) (1981) 363–369.
[5] V.V. Molkov, Theoretical generalization of international experimental data on vented explosion dynamics, in: V.V. Molkov (Ed.), Proceedings of the First International Seminar on Fire and Explosion Hazards (17–21 July 1995, Moscow, Russia), All-Russian Research Institute for Fire Protection—Russian Association for Fire Safety Science, 1995, pp. 166–181.
[6] D.M. Razus, U. Krause, Comparison of empirical and semi-empirical calculation methods for venting of gas explosions, Fire Saf. J. 36 (2001) 1–23.
[7] T. Hirano, Combustion Science for Safety, in: J.H. Chen, M.D. Colket (Eds.), Proceedings of 29th International Symposium on Combustion, July 21–25, 2002, Sapporo, Japan), The Combustion Institute, Pittsburgh, 2002, pp. 167–180.
[8] F. Williams, Approaches to the scaling of fires and explosions through mechanistic considerations, in: D. Bradley, D. Drysdale, V. Molkov (Eds.), Proceedings of the Fourth International Seminar on Fire and Explosion Hazards, Londonderry, Northern Ireland, UK, September 8–12, 2003, pp. 445–456.
[9] V.V. Molkov, A.Ya. Korolchenko, S.V. Alexandrov, Venting of deflagrations in buildings and equipment: universal correlation, in: Y. Hasemi (Ed.), Proceedings of the Fifth International Symposium on Fire Safety Science, Melbourne, Australia, March 3–7, 1997, pp. 1249–1260.
[10] A. Di Benedetto, E. Salzano, G. Russo, Analysis of pressure piling by means of empirical correlation for vented vessels, in: D.

Bradley, D. Drysdale, V. Molkov (Eds.), Proceedings of the Fourth International Seminar on Fire and Explosion Hazards, Londonderry, Northern Ireland, UK, September 8–12, 2003, pp. 413–424.
[11] V.V. Molkov, Unified correlations for vent sizing of enclosures against gaseous deflagrations at atmospheric and elevated pressures, J. Loss Prev. Process Industries 14 (2001) 567–574.
[12] V.V. Molkov, Explosion safety engineering: NFPA 68 and improved vent sizing technology, in: Interflam 1999, Proceedings of the Eighth International Fire Science Conference, June 29–July 1, 1999, Edinburgh Conference Centre, Scotland, pp. 1129–1134.
[13] NFPA 68, Guide for Venting of Deflagrations, 2002 Edition, National Fire Protection Association, USA, 2002.
[14] V.V. Molkov, A.V. Grigorash, F. Tamanini, R. Dobashi, R.M. Eber, Vented gaseous deflagrations: modelling of translating inertial vent covers, J. Loss Prev. Process Industries 16 (5) (2003) 395–402.
[15] V.V. Molkov, Venting of Gaseous Deflagrations, in: DSc Dissertation, VNIIPO, Moscow, Russia, 1996 (in Russian).
[16] A. Grigorash, R. Eber, V. Molkov, A theoretical model of vented gaseous deflagrations in enclosures with inertial vent covers, in: D. Bradley, D. Drysdale, V. Molkov (Eds.), Proceedings of the Fourth International Seminar on Fire and Explosion Hazards, Londonderry, Northern Ireland, UK, September 8–12, 2003, pp. 445–456.
[17] S. Höchst, W. Leuckel, On the effect of venting large vessels with mass inert panels, J. Loss Prev. Process Industries 11 (1998) 89–97.
[18] R.G. Zalosh, Gas explosion tests in room-size vented enclosures, in: Proceedings of AIChE Loss Prevention Symposium, 1978, pp. 98–110.